IEEE Access
Multidisciplinary ⋮ Rapid Review ⋮ Open Access Journal

Received August 22, 2020, accepted September 20, 2020, date of publication October 21, 2020, date of current version November 6, 2020.

Digital Object Identifier 10.1109/ACCESS.2020.3032836

Preliminary Study on Double Enhanced Raman Scattering Detection of Gas Phase Trace Explosives

ZHIBIN CHEN[1,2], MENGZE QIN[1,2], AND CHENG XIAO[3]

[1]Department of Electronics and Optical Engineering, Army Engineering University at Shijiazhuang Campus, Shijiazhuang 050003, China
[2]32181 Unit of PLA, Shijiazhuang 050003, China
[3]China Satellite Maritime Tracking and Controlling Department, Jiangyin 214400, China

Corresponding author: Zhibin Chen (shangxinboy@163.com)

This work was supported by the National Defense Research Program of Science and Technology, China, under Grant 2004053.

ABSTRACT The demand of continuous detection technology for gas phase trace explosives (GPTE) in explosion-proof stability maintenance, public security, explosive security storage and other occasions is summarized. By studying the development status and research trends of surface enhanced Raman scattering (SERS) detection technology to detect GPTE, an application of a double enhanced Raman scattering (DERS) substrate consisted of a novel 1D composite silver grating and gold nanospheres colloids in the GPTE detection was presented. The detection sensitivity of 2,4,6-trinitrotoluene (TNT) and cyclotrimethyltrinitroamine (RDX) was 10^{-11} mol/L. Combining with microfluidic technology, it can realize in-situ and continuous GPTE detection. This DERS substrate has a significant reference for the application of SERS detection technology in food safety, health care and environmental monitoring, *et al.*

INDEX TERMS Composite sinusoidal grating, continuous detection, gas phase trace explosives, gold nanoparticles colloids, surface enhanced Raman scattering.

I. INTRODUCTION

In recent years, with the increasingly rampant global terrorist activities and the gradual intensification of local regional conflicts, a large number of hidden explosives, such as time bombs, landmines and other forms of explosive devices, are threatened in the process of peacekeeping, stability maintenance and riot handling. Therefore, it is necessary to search and locate these hidden explosives. In the subway, airport, station, shopping mall and other public security work, also need to carry out explosive ordnance. With the emergence of new types of explosives, in the process of explosive storage, explosives need to be classified and arranged, safety monitoring and early warning [1]–[3]. At the same time, these explosives, in addition to the risk of severe explosion, also pose an important threat to environmental safety. Leakage in the natural environment often occurs in production, manufacturing and transportation, which requires real-time monitoring. A high sensitivity, fast, portable, easy to operate, and continuous detection of GPTE detection instrument is urgently needed to complete these detection and monitoring work.

Traditional trace explosive detection technology mainly includes spectroscopic technology, chemical reaction sensor technology and biosensor technology. These technologies have problems such as large equipment quality and volume, inability to continuously repeat sampling, poor environmental adaptability, low selectivity, and environmental pollution [4]–[11].

Surface enhanced Raman scattering (SERS) detection technology has become a trend and hot spot in the field of trace explosives detection because it can recognize the structural information of substances at the molecular level, and has high detection sensitivity (or even single molecule detection) and high selectivity. At the same time, it has the characteristics of small interference by water, quenching fluorescence, good stability and so on [12], [13].

The key to realize SERS detection of trace explosives was to study a SERS substrate with simple preparation process, good reproducibility and continuous detection. According to the specific functional structure and characteristics of SERS substrate, it can be divided into the following five

The associate editor coordinating the review of this manuscript and approving it for publication was Mira Naftaly.

categories: (1) SERS substrate with rough noble metal [14]–[20]; (2) SERS substrate with periodic array structure [21]–[24]; (3) SERS substrate with assembled ordered particle [25]–[28]; (4) Core shell SERS substrate [29]–[32]; (5) Graphene composite SERS substrate [33]–[38]. Two novel SERS substrates with special functions, diatom cell environmental protection substrate [39] and photocatalytic self-cleaning substrate [40], were also introduced in the literatures. To a certain extent, these substrates can realize the detection of GPTE with high detection sensitivity. But there are still some defects such as complex processing technology, poor reproducibility, memory effect and poor reusability.

A double enhanced Raman scattering (DERS) substrate for detection of GPTE is proposed. The substrate is based on the coupling between the SPP of silver sinusoidal grating (AgSG) and the LSP of gold nanoparticles (AuNPs). The substrate has the characteristics of simple preparation, good reproducibility and continuous detection. Combined with microfluidic technology, continuous and real-time detection of GPTE can be realized.

II. STRUCTURAL DESIGN OF DERS SUBSTRATE

Continuous repeatable detection has always been a difficult problem in the SERS detection field, which is of great significance to reduce the cost of SERS detection and improve the efficiency of SERS detection, and realize online continuous detection. Especially during the extensive application of SERS detection technology and microflow control technology, continuous repeated detection is particularly important.

The key to continuous SERS detection of GPTE is that the substrate has a sufficiently high enhancement factor (EF) to achieve high-sensitivity detection and there is no ''memory effect'' [41], that is, explosive molecules are not easily adsorbed on the surface of the substrate.

In this paper, a kind of DERS substrate with AgSG and AuNPs colloids is proposed. Combined with microfluidic technology, the GPTE can be continuously detected by SERS, as shown in FIGURE 1. AuNPs colloids can adsorb the explosive molecules in the air. Moreover, AuNPs and explosives are not easy to adsorb on the surface of AgSG. The DERS substrate is integrated into the open microchannel to keep the AuNPs colloid flowing continuously in the micro channel. The GPTE can be continuously sampled to achieve high sensitivity and continuous SERS detection of the DERS substrate for airborne explosive molecules.

A. SILVER SINUSOIDAL GRATING SERS SUBSTRATE

In the process of studying the AgSG structure, the Finite Difference Time Domain (FDTD) simulation method was adopted. In order to obtain the optimal grating structure, the grating parameters (period P, silver thickness d and sinusoidal amplitude A) are studied in detail. The working wavelengths used in the simulation are 532 nm and 785 nm, which are the corresponding working wavelengths of Raman spectrometer and other supporting equipment commonly used in the field of SERS detection of explosives.

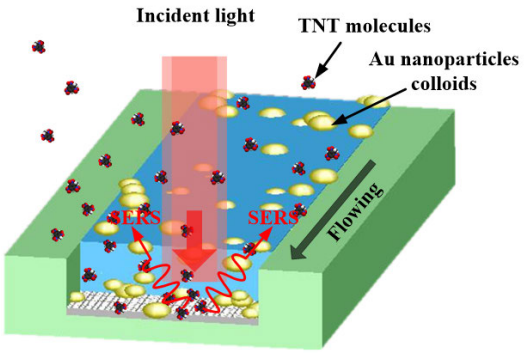

FIGURE 1. Schematic diagram of gas phase trace explosives detected by substrate.

Assuming that the amplitude of the sinusoidal curve of the silver grating is 50nm, the enhancement factor of the grating under different periods and different thickness of silver layer was simulated and calculated. As shown in Table 1, the selected thickness of silver layer ranges from 20 to 200 nm, and the grating period ranges from 450 to 1540 nm.

The structure parameters of grating have great influence on the EF of SERS. It can be seen from TABLE 1 that when the sinusoidal amplitude of the grating is 50 nm, the EF can reach 10^3 by optimizing the grating period and the thickness of silver layer. Therefore, in order to obtain the maximum EF of SERS, the optimal matching relationship between the grating period, the thickness of silver layer and the wavelength of incident light must be considered.

FIGURE 2 shows a two-dimensional gray scale diagram of the absorbance of incident light corresponding to four kinds of gratings with different periods varying with the wavelength of incident light and the thickness of silver layer. The gray value in the image represents the absorbance. In the corresponding response wavelength region, when the thickness of silver layer is greater than 50 nm, the absorbance remains basically unchanged, so the thickness of silver layer is set to 100 nm in the next simulation.

In addition, it can be found that there is a strong absorbance region near the incident wavelength of 400 nm. This is not the light absorption caused by exciting the surface SPP resonance wave, but the reason that silver naturally absorbs light in this wavelength region relatively strongly. The shorter the wavelength of the incident light, the stronger the natural absorption of silver. Therefore, for the 1D AgSG substrate, the wavelength of the incident light is selected to be 785 nm.

In order to further analyze the situation when the incident wavelength is 785nm, the relationship between the absorbance of the grating with four periods and the thickness of silver layer when the wavelength is 785nm is shown in FIGURE 3 (a). When the grating period is 770nm, the absorbance is the largest. When the thickness of silver layer is greater than 70nm, the absorbance is basically maintained at 0.17. This is because when the thickness of silver layer continues to increase, the reflection of incident light plays a

TABLE 1. Enhanced factor at two excitation wavelengths as a function of silver layer thickness and grating period.

λ (nm)	d (nm)	P(nm)							
		450	505	700	770	950	1010	1300	1540
532	20	237	515	18	18	18	18	18	18
	40	408	520	31	32	26	96	32	27
	80	807	1552	37	37	38	424	38	30
	100	841	1640	37	37	40	441	38	30
	120	847	1726	36	36	40	445	37	29
	160	900	1665	34	34	38	441	34	28
	180	841	1655	32	31	37	441	32	27
	200	841	1624	31	30	37	437	31	27
785	20	20	14	202	454	25	27	24	24
	40	23	26	237	4489	31	32	31	185
	80	22	27	231	8464	26	29	32	534
	100	23	27	231	8649	22	23	27	566
	120	23	27	231	8649	22	22	22	581
	160	24	28	234	8464	22	22	22	576
	180	24	28	234	8281	22	22	22	566
	200	24	28	234	8100	21	22	22	566

leading role. When the thickness of silver layer is less than 70nm, the absorbance changes rapidly, so it is reasonable to choose the optimized thickness of the silver layer to be 100nm.

As can be seen in FIGURE 3 (b), there are two absorbance peaks ($\lambda = 435$nm and 790nm) when the grating period is 770nm. Moreover, at these two corresponding wavelengths, the grating with a period of 770 nm has the highest absorbance. This shows that when the wavelength is 785nm, the matching optimized grating period is 770nm, that is, the 1D AgSG with the corresponding period of the surface SPP resonance wave has the largest surface electric field enhancement. The grating period plays an important role in the generation of SPP resonance waves.

The amplitude of the AgSG is another parameter that plays an important role in the formation of SPP resonance waves. FIGURE 3 (c) shows the relationship between the absorbance of four AgSGs with different amplitudes and the thickness of silver layer when the incident wavelength is 785nm and the grating period is 770nm. When the amplitude is 15nm, the grating absorbance is larger. It can be obtained from TABLE 2 that when the amplitude is 15 nm, the SERS enhancement factor has a maximum value. When the thickness of the silver layer is greater than 75nm, the light absorption rate of the grating remains basically unchanged, which also shows the rationality of choosing the grating to optimize the thickness of silver layer to 100nm.

TABLE 2. EF as a function of amplitude of AgSG.

d(nm)	SERS enhancement factor
10	91204
15	122283
20	96100
25	66564
40	17424
50	8649

It can be seen from Figure 6 that there is an absorbance peak at the incident light wavelength of 790 nm, and the absorbance peak does not change with the amplitude. According to TABLE 2, by optimizing the grating amplitude, the SERS enhancement factor can reach the order of 10^5.

According to the above structural optimization analysis, the specific structural parameters of the optimized SERS substrate matched with $\lambda = 785$nm are: $P = 770$nm, $d = 100$nm and $A = 15$nm.

B. SPP&LSP COUPLING OF DERS SUBSTRATE

Through FDTD simulation, the EF of SERS substrate based on AgSG can reach 10^5. It is difficult to meet the needs of trace detection. In order to improve the EF of the substrate, a kind of DERS substrate was formed by combining AuNPs colloids on the surface of AgSG. The SERS substrate

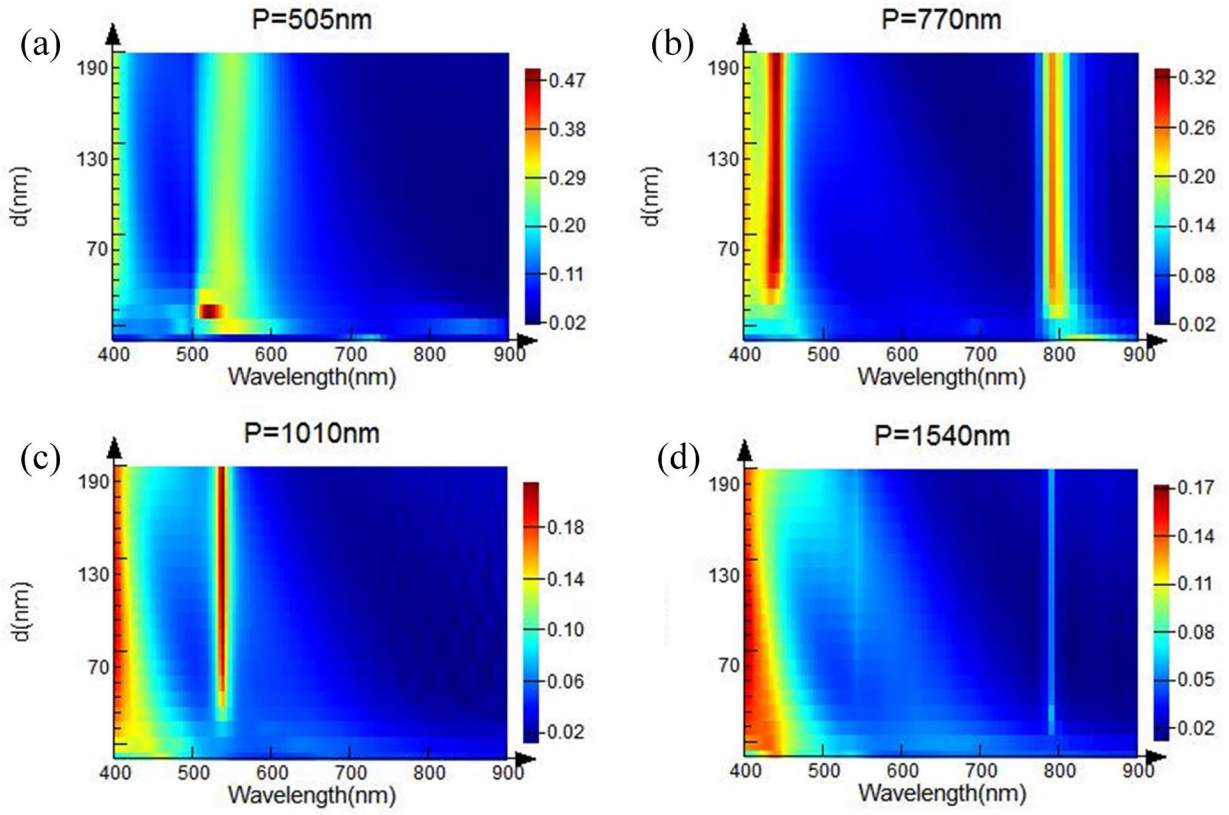

FIGURE 2. Absorbance as a function of incident light wavelength and Ag layer thickness with different periods: (a) P = 505nm; (b) P = 770nm; (c) P = 1010nm; (d) P = 1540nm.

effectively solves the problem of weak Raman enhancement ability of single AgSG.

The electric field enhancement region between AuNPs is formed by LSP. Through the coupling between LSP and SPP on the surface of AgSG, the electric field strength between AuNPs is further enhanced. As a result, the number and range of hot spots per unit volume on the DERS substrate are increased, resulting in stronger Raman signals. AuNPs can adsorb trace explosive molecules to form dimer, trimer and other polymers. The EF formed by the coupling effect of LSP and SPP can reach 10^9. In order to excite the SPP-LSP coupling effect in DERS substrate, AuNPs need to sink into the SERS long range region of AgSG. In the actual detection process, appropriate amount of NaCl can be added into the colloidal to promote the formation of AuNPs aggregate and sink to the surface of the grating.

III. POLARIZATION-INDEPENDENT DERS SUBSTRATE

A. POLARIZATION DEPENDENCE OF 1D AgSG SERS SUBSTRATE

Currently, the laser light source used in the SERS detection field is usually linearly polarized light. The 1D AgSG SERS substrate is very sensitive to the polarization direction of the incident light. That is, the incident light has an optimal polarization direction, and the strongest SERS signal can be detected only when the incident light is incident in this polarization direction.

In order to study the enhancement ability of the 1D AgSG SERS substrate, the polarization angle of the incident light source was scanned in the range of 0∼90° and the wavelength of the incident light in the range of 400∼900nm using FDTD software. The scanning step of the polarization angle is 5°, and the scanning step of the incident wavelength is 2 nm. Obtain the absorbance of the substrate under different wavelengths and polarization angles, as shown in Figure 4, where the gray value in the figure represents the absorbance. The polarization angle of the incident light has a great influence on the absorbance. Especially at the incident wavelength of 785nm, when the polarization angle is 0° (the polarization direction is perpendicular to the groove of the grating), the absorbance has a maximum value, and the SERS effect is the strongest.

In addition, the relationship between the absorbance and the polarization angle is analyzed when the incident light wavelength is 785 nm. As shown in FIGURE 5, the absorbance curve is highly like that of $b\cos^2\alpha$ function, where b is a constant and α is the polarization angle of incident light.

Since the SERS enhancement factor of the 1D AgSG is very sensitive to the polarization angle of the incident light, in order to obtain the strongest SERS response, the

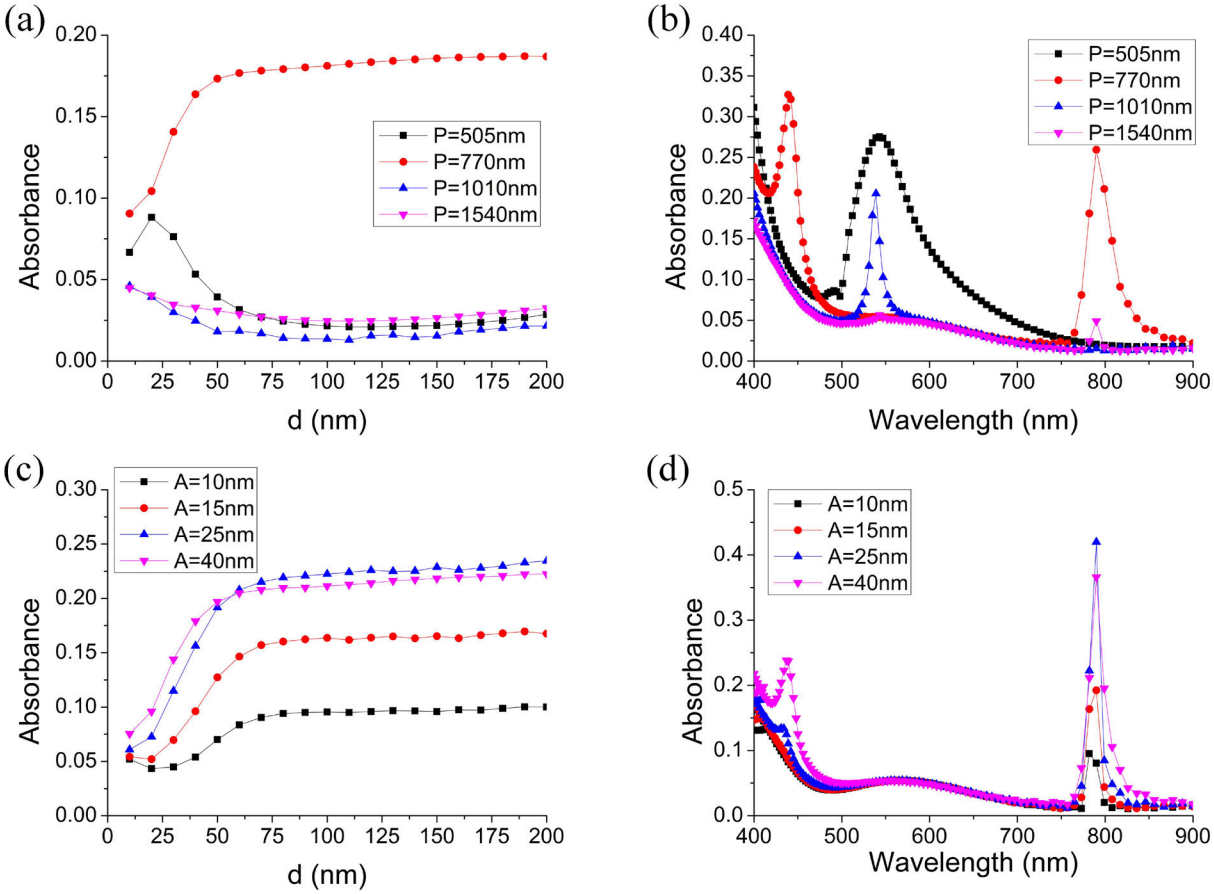

FIGURE 3. (a) Absorbance as a function of Ag layer thickness with different periods at $\lambda = 785$nm; (b) Absorbance as a function of incident light wavelength with different periods at $d = 100$nm; (c) Absorbance as a function of Ag layer thickness with different amplitudes at $\lambda = 785$nm; (d) Absorbance as a function of incident light wavelength with different amplitudes at $d = 100$nm.

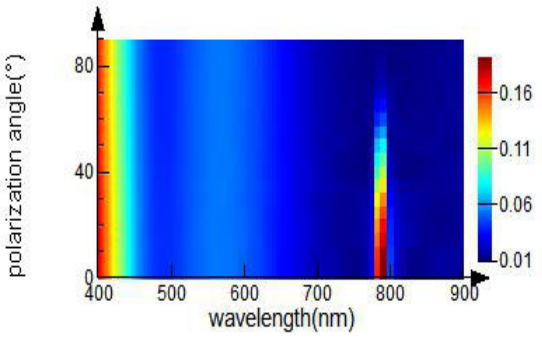

FIGURE 4. Absorbance as a function of incident light wavelength and polarization angle.

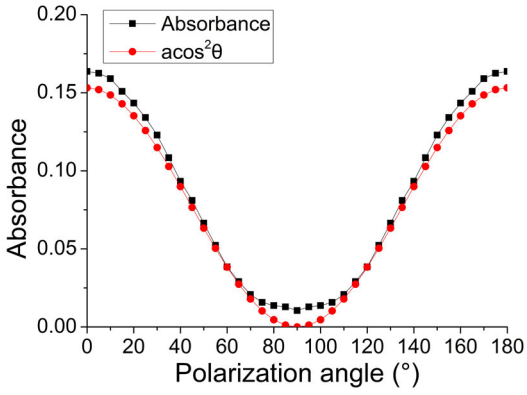

FIGURE 5. Absorbance as a function of polarization angle.

polarization angle of the incident light must be 0°. That is, the polarization direction of the incident light and the groove direction of grating must be kept perpendicular to each other, which will cause inconvenience in the actual SERS detection application process.

B. POLARIZATION-INDEPENDENT DERS SUBSTRATE

In order to overcome the polarization dependence of 1D AgSG substrate, a polarization-independent 2D AgSG substrate is proposed. The substrate can be easily fabricated by Maskless Laser interference lithography, which makes it possible to prepare SERS substrate with low cost, large area and good reproducibility.

The structure of the 2D AgSG is shown in FIGURE 6, which can be regarded as the superposition of two 1D AgSG

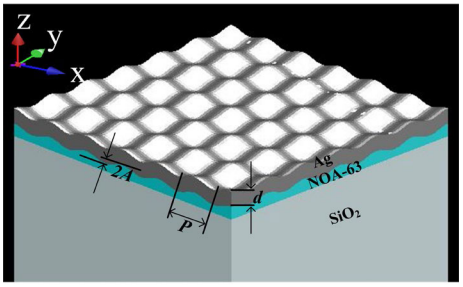

FIGURE 6. Schematic diagram of 2D AgSG.

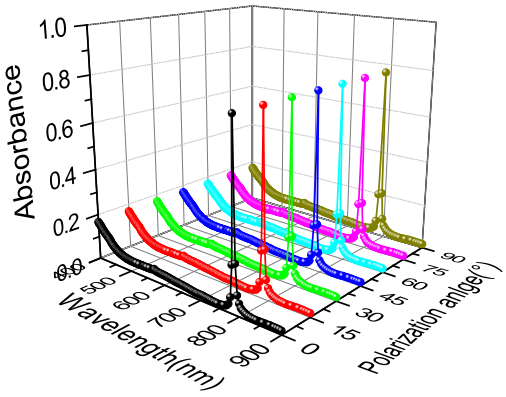

FIGURE 7. Absorbance as a function of incident light wavelength and polarization angle.

in vertical directions. The 2D AgSG has a period of 770 nm in X and Y directions, a sinusoidal amplitude of 15 nm and a silver layer thickness of 100 nm. The substrate consists of silver, cured photoresist and silica. The light gray part is silica layer, the light blue part is photoresist (XAR-N7730/30) layer, and the dark gray part is silver layer.

The polarization angle of the incident light is in the range of 0∼90° and the wavelength of the incident light is in the range of 400∼900 nm. The scanning step of polarization angle is 15° and the scanning step of incident light wavelength is 2nm. The absorbance of 2D AgSG under different incident wavelength and polarization angle is obtained. When the polarization angle of the incident light is equal to 0, 15, 30, 45, 60, 75 and 90 degrees, the 2D AgSG has an absorption peak at 786 nm. Due to the structural symmetry of the 2D AgSG, it is easy to find that the same absorption peak can be obtained in the range of polarization angle of 90∼360°. This is consistent with the design requirement of 785nm.

Similarly, the 2D DERS substrate can be formed by SPP-LSP between the 2D sinusoidal silver grating and gold nanoparticles colloids. Based on the high sensitivity and no ''memory effect'' of 1D DERS substrate, the substrate overcomes the polarization dependence and is polarization independent.

C. PERFORMANCE TESTING

2D AgSG was fabricated in the laboratory. The SEM image of the surface morphology of the grating is shown in FIGURE 8(a), with a period of 770nm and a depth of about 34nm. AuNPs colloids with a diameter of about 95nm was prepared by sodium citrate reduction method. The TEM diagram is shown in FIGURE 8(b).

The polarization independent DERS substrate was obtained by combining the 2D AgSG with AuNPs colloids. The SERS detection of low concentration TNT solution and RDX solution without molecular recognition reagent was carried out using the substrate. Firstly, ethanol was used as the solvent to prepare TNT solution and RDX solution samples with concentrations of 10^{-9} mol/L, 10^{-10} mol/L and 10^{-11} mol/L respectively. TNT solution and RDX solution were added to the DERS substrate without any molecular recognition reagent. The SERS spectra of TNT and RDX were collected, as shown in FIGURE 9. The detection concentration of TNT solution and RDX solution is 10^{-11} mol/L on the polarization independent DERS substrate. Many kinds of explosive molecules can be detected by using the DERS substrate. In the next research work, more common typical explosives will be detected, and a more perfect comparison Library of trace explosives Raman spectra will be established.

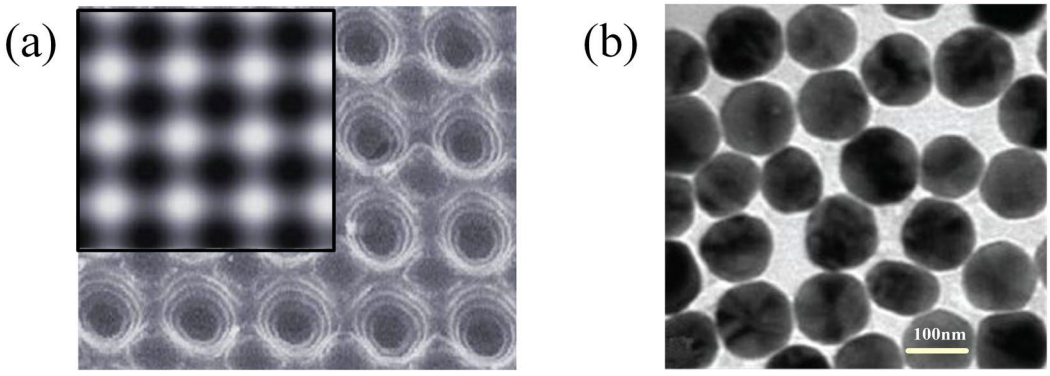

FIGURE 8. (a) SEM of 2D AgSG; (b) TEM of AuNPs colloids.

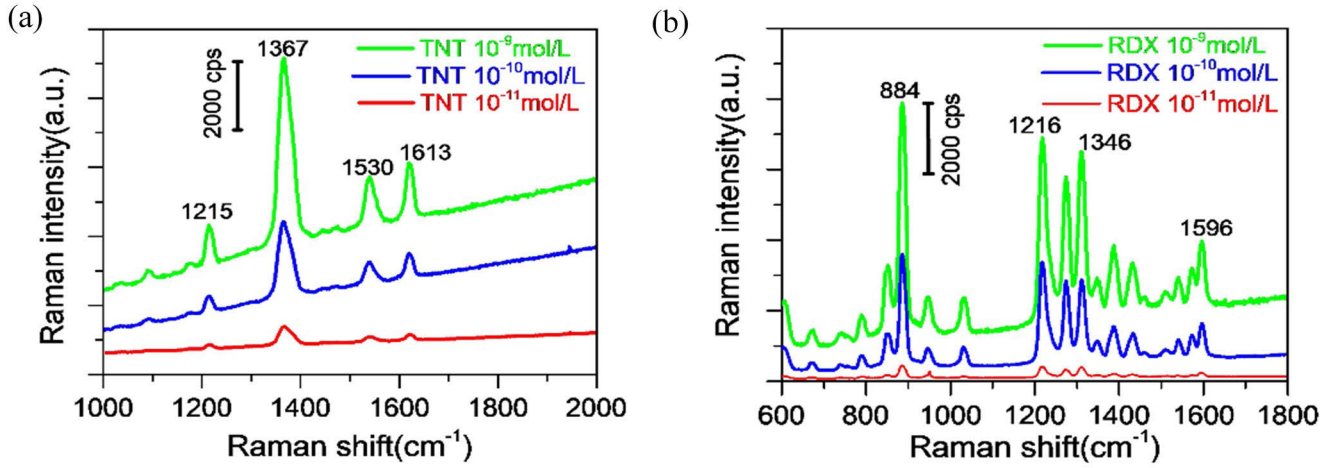

FIGURE 9. **(a) SERS spectra of TNT; (b) SERS spectra of RDX.**

In addition, the continuous sampling detection performance of the DERS substrate was tested. The "memory effect" could be eliminated by the continuous flow of AuNPs colloids on the grating surface, and the Raman signal of TNT could not be detected on the DERS substrate.

IV. CONCLUSION

In this paper, a kind of continuous detection DERS substrate combined with microfluidic technology is proposed. Microfluidic technology is used to sample the trace explosive molecules, and the continuous flow of metal nanospheres in the microchannel is used to realize the continuous sampling of trace explosives. This technology has laid a technical foundation for providing a high-sensitivity portable continuous detection device for trace explosives, to realize trace, continuous, fast, portable, stable and environmental detection of trace explosives. In addition, trace material detection technology is also needed in environmental monitoring, food safety and medical inspection. Therefore, the research on this technology is of great significance to enrich and optimize the current trace material detection technology and will promote the in-depth development of trace material detection technology.

REFERENCES

[1] J. S. Caygill, F. Davis, and S. P. J. Higson, "Current trends in explosive detection techniques," *Talanta*, vol. 88, pp. 14–29, Jan. 2012, doi: 10.1016/j.talanta.2011.11.043.

[2] A. Hakonen, P. O. Andersson, M. S. Schmidt, T. Rindzevicius, and M. Käll, "Explosive and chemical threat detection by surface-enhanced Raman scattering: A review," *Anal. Chim. Acta*, vol. 893, pp. 1–13, Sep. 2015, doi: 10.1016/j.aca.2015.04.010.

[3] M. López-López and C. García-Ruiz, "Infrared and Raman spectroscopy techniques applied to identification of explosives," *TrAC Trends Anal. Chem.*, vol. 54, pp. 36–44, Feb. 2014, doi: 10.1016/j.trac.2013.10.011.

[4] Y. Zhao, M. Pan, F. Liu, Y. Liu, P. Dong, J. Feng, T. Shi, and X. Liu, "Highly selective and sensitive detection of trinitrotoluene by framework-enhanced fluorescence of gold nanoclusters," *Anal. Chim. Acta*, vol. 1106, pp. 133–138, Apr. 2020, doi: 10.1016/j.aca.2020.01.055.

[5] B. Gilbert-López, F. J. Lara-Ortega, J. Robles-Molina, S. Brandt, A. Schütz, D. Moreno-González, J. F. García-Reyes, A. Molina-Díaz, and J. Franzke, "Detection of multiclass explosives and related compounds in soil and water by liquid chromatography-dielectric barrier discharge ionization-mass spectrometry," *Anal. Bioanal. Chem.*, vol. 411, no. 19, pp. 4785–4796, Jul. 2019.

[6] L. E. DeGreeff, H. P. H. Liddell, W. R. Pogue, M. H. Merrill, and K. J. Johnson, "Effect of re-use of surface sampling traps on surface structure and collection efficency for trace explosive residues," *Forensic Sci. Int.*, vol. 297, pp. 254–264, Apr. 2019.

[7] C. Costa, E. M. van Es, P. Sears, J. Bunch, V. Palitsin, H. Cooper, and M. J. Bailey, "Exploring a route to a selective and sensitive portable system for explosive detection—Swab spray ionisation coupled to of high-field assisted waveform ion mobility spectrometry (FAIMS)," *Forensic Sci. Int., Synergy*, vol. 1, pp. 214–220, Jan. 2019.

[8] C. Costa, E. M. van Es, P. Sears, J. Bunch, V. Palitsin, K. Mosegaard, and M. J. Bailey, "Exploring rapid, sensitive and reliable detection of trace explosives using paper spray mass spectrometry (PS–MS)," *Propellants, Explosives, Pyrotechnics*, vol. 44, no. 8, pp. 1021–1027, Aug. 2019, doi: 10.1002/prep.201800320.

[9] M. Mullen and B. C. Giordano, "Part per quadrillion quantitation of pentaerythritol tetranitrate vapor using online sampling gas chromatography–mass spectrometry," *J. Chromatogr. A*, vol. 1603, pp. 407–411, Oct. 2019, doi: 10.1016/j.chroma.2019.05.029.

[10] M. Amo-González, S. Pérez, R. Delgado, G. Arranz, and I. Carnicero, "Tandem ion mobility spectrometry for the detection of traces of explosives in cargo at concentrations of parts per quadrillion," *Anal. Chem.*, vol. 91, no. 21, pp. 14009–14018, 2019.

[11] W. Zhang, Y. Tang, A. Shi, L. Bao, Y. Shen, R. Shen, and Y. Ye, "Recent developments in spectroscopic techniques for the detection of explosives," *Materials*, vol. 11, no. 8, p. 1364, Aug. 2018.

[12] D.-W. Li, W.-L. Zhai, Y.-T. Li, and Y.-T. Long, "Recent progress in surface enhanced Raman spectroscopy for the detection of environmental pollutants," *Microchim. Acta*, vol. 181, nos. 1–2, pp. 23–43, Jan. 2014, doi: 10.1007/s00604-013-1115-3.

[13] S. Almaviva, S. Botti, L. Cantarini, A. Palucci, A. Puiu, A. Rufoloni, L. Landstrom, and F. S. Romolo, "Trace detection of explosives by surface enhanced Raman spectroscopy," *Proc. SPIE*, vol. 8546, Oct. 2012, Art. no. 854602.

[14] M. Sun, H. Qian, J. Liu, Y. Li, S. Pang, M. Xu, and J. Zhang, "A flexible conductive film prepared by the oriented stacking of ag and Au/Ag alloy nanoplates and its chemically roughened surface for explosive SERS detection and cell adhesion," *RSC Adv.*, vol. 7, no. 12, pp. 7073–7078, 2017, doi: 10.1039/C6RA25956A.

[15] P. R. Sajanlal and T. Pradeep, "Functional hybrid nickel nanostructures as recyclable SERS substrates: Detection of explosives and biowarfare agents," *Nanoscale*, vol. 4, no. 11, p. 3427, 2012, doi: 10.1039/c2nr30557g.

[16] S. Emamian, A. Eshkeiti, B. B. Narakathu, S. G. R. Avuthu, and M. Z. Atashbar, "Gravure printed flexible surface enhanced Raman spectroscopy (SERS) substrate for detection of 2,4-dinitrotoluene (DNT) vapor," *Sens. Actuators B, Chem.*, vol. 217, pp. 129–135, Oct. 2015.
[17] P. M. Fierro-Mercado and S. P. Hernández-Rivera, "Highly sensitive filter paper substrate for SERS trace explosives detection," *Int. J. Spectrosc.*, vol. 2012, pp. 1–7, Oct. 2012, doi: 10.1155/2012/716527.
[18] A. Chou, E. Jaatinen, R. Buividas, G. Seniutinas, S. Juodkazis, E. L. Izake, and P. M. Fredericks, "SERS substrate for detection of explosives," *Nanoscale*, vol. 4, no. 23, pp. 7419–7424, 2012.
[19] J. M. Sylvia, J. A. Janni, J. D. Klein, and K. M. Spencer, "Surface-enhanced Raman detection of 2,4-dinitrotoluene impurity vapor as a marker to locate landmines," *Anal. Chem.*, vol. 72, no. 23, pp. 5834–5840, Dec. 2000, doi: 10.1021/ac0006573.
[20] J. Lee, B. Hua, S. Park, M. Ha, Y. Lee, Z. Fan, and H. Ko, "Tailoring surface plasmons of high-density gold nanostar assemblies on metal films for surface-enhanced Raman spectroscopy," *Nanoscale*, vol. 6, no. 1, pp. 616–623, 2014.
[21] E. L. Holthoff, D. N. Stratis-Cullum, and M. E. Hankus, "A nanosensor for TNT detection based on molecularly imprinted polymers and surface enhanced Raman scattering," *Sensors*, vol. 11, no. 3, pp. 2700–2714, 2011, doi: 10.3390/s110302700.
[22] S. Chang, H. Ko, S. Singamaneni, R. Gunawidjaja, and V. V. Tsukruk, "Nanoporous membranes with mixed nanoclusters for Raman-based label-free monitoring of peroxide compounds," *Anal. Chem.*, vol. 81, no. 14, pp. 5740–5748, Jul. 2009, doi: 10.1021/ac900537d.
[23] H. Ko, S. Chang, and V. V. Tsukruk, "Porous substrates for label-free molecular level detection of nonresonant organic molecules," *ACS Nano*, vol. 3, no. 1, pp. 181–188, Jan. 2009, doi: 10.1021/nn800569f.
[24] H. Zhou, Z. Zhang, C. Jiang, G. Guan, K. Zhang, Q. Mei, R. Liu, and S. Wang, "Trinitrotoluene explosive lights up ultrahigh Raman scattering of nonresonant molecule on a top-closed silver nanotube array," *Anal. Chem.*, vol. 83, no. 18, p. 6913, 2011.
[25] T. F. Chen, S. H. Lu, A. J. Wang, D. Zheng, Z. L. Wu, and Y. S. Wang, "Detection of explosives by surface enhanced Raman scattering using substrate with a monolayer of ordered Au nanoparticles," *Appl. Surf. Sci.*, vol. 317, pp. 940–945, Oct. 2014, doi: 10.1016/j.apsusc.2014.09.015.
[26] R. Sardar, T. Liyanage, A. Rael, S. Shaffer, S. Zaidi, and J. V. Goodpaster, "Fabrication of a self-assembled and flexible SERS nanosensor for explosive detection at parts-per-quadrillion levels from fingerprints," *Analyst*, vol. 143, no. 9, pp. 2012–2022, 2018.
[27] X. Liu, L. Zhao, H. Shen, H. Xu, and L. Lu, "Ordered gold nanoparticle arrays as surface-enhanced Raman spectroscopy substrates for label-free detection of nitroexplosives," *Talanta*, vol. 83, no. 3, pp. 1023–1029, Jan. 2011, doi: 10.1016/j.talanta.2010.11.015.
[28] J. Wang, L. Yang, S. Boriskina, B. Yan, and B. M. Reinhard, "Spectroscopic ultra-trace detection of nitroaromatic gas vapor on rationally designed two-dimensional nanoparticle cluster arrays," *Anal. Chem.*, vol. 83, no. 6, pp. 2243–2249, Mar. 2011, doi: 10.1021/ac103123r.
[29] F. A. Calzzani, A. Kassu, J. M. Taguenang, A. Sharma, P. B. Ruffin, and C. Brantley, "Detection of residual traces of explosives by surface enhanced Raman scattering using gold coated substrates produced by nanospheres imprint technique," *Proc. SPIE*, vol. 6945, Apr. 2008, Art. no. 69451O.
[30] H. X. Gu, L. Xue, Y. H. Zhang, Y. F. Zhang, and L. Y. Cao, "Functionalized gold nanoparticles coated polymer spheres as SERS substrate for the detection of TNT explosives," *Adv. Mater. Res.*, vol. 924, pp. 366–370, Apr. 2014, doi: 10.4028/www.scientific.net/AMR.924.366.
[31] K. Qian, H. Liu, L. Yang, and J. Liu, "Functionalized shell-isolated nanoparticle-enhanced Raman spectroscopy for selective detection of trinitrotoluene," *Analyst*, vol. 137, no. 20, p. 4644, 2012, doi: 10.1039/c2an35947b.
[32] E. De La Cruz-Montoya, G. Pérez-Acosta, T. L. Pineda, and S. P. Hernández-Rivera, "Surface enhanced Raman scattering of TNT and DNT on colloidal nanoparticles of Ag/TiO_2," *Proc. SPIE*, vol. 6538, no. 4, pp. 337–342, 2007.
[33] M. Liu and W. Chen, "Graphene nanosheets-supported Ag nanoparticles for ultrasensitive detection of TNT by surface-enhanced Raman spectroscopy," *Biosensors Bioelectron.*, vol. 46, pp. 68–73, Aug. 2013, doi: 10.1016/j.bios.2013.01.073.
[34] R. Kanchanapally, S. S. Sinha, Z. Fan, M. Dubey, E. Zakar, and P. C. Ray, "Graphene oxide–gold nanocage hybrid platform for trace level identification of nitro explosives using a Raman fingerprint," *J. Phys. Chem. C*, vol. 118, no. 13, pp. 7070–7075, Apr. 2014, doi: 10.1021/jp5015548.
[35] X. Xiu, Y. Guo, C. Li, Z. Li, D. Li, C. Zang, S. Jiang, A. Liu, B. Man, and C. Zhang, "High-performance 3D flexible SERS substrate based on graphene oxide/silver nanoparticles/pyramid PMMA," *Opt. Mater. Express*, vol. 8, no. 4, p. 844, Apr. 2018, doi: 10.1364/OME.8.000844.
[36] C. X. Guo, Y. Lei, and C. M. Li, "Porphyrin functionalized graphene for sensitive electrochemical detection of ultratrace explosives," *Electroanalysis*, vol. 23, no. 4, pp. 885–893, Apr. 2011, doi: 10.1002/elan.201000522.
[37] X. Ling, J. Wu, W. Xu, and J. Zhang, "Probing the effect of molecular orientation on the intensity of chemical enhancement using graphene-enhanced Raman spectroscopy," *Small*, vol. 8, no. 9, pp. 1365–1372, May 2012.
[38] Y. Zhao, X. Li, Y. Du, G. Chen, Y. Qu, J. Jiang, and Y. Zhu, "Strong light–matter interactions in sub-nanometer gaps defined by monolayer graphene: Toward highly sensitive SERS substrates," *Nanoscale*, vol. 6, no. 19, pp. 11112–11120, 2014, doi: 10.1039/c4nr03152k.
[39] X. Kong, Y. Xi, P. Le Duff, X. Chong, E. Li, F. Ren, G. L. Rorrer, and A. X. Wang, "Detecting explosive molecules from nanoliter solution: A new paradigm of SERS sensing on hydrophilic photonic crystal biosilica," *Biosensors Bioelectron.*, vol. 88, pp. 63–70, Feb. 2017.
[40] K. Xu, H. Yan, C. F. Tan, Y. Lu, Y. Li, G. W. Ho, R. Ji, and M. Hong, "Hedgehog inspired CuO Nanowires/Cu_2O composites for broadband visible-light-driven recyclable surface enhanced Raman scattering," *Adv. Opt. Mater.*, vol. 6, no. 7, Apr. 2018, Art. no. 1701167, doi: 10.1002/adom.201701167.
[41] B. Sharma, F. Cardinal, S. L. Kleinman, N. G. Greeneltch, R. R. Frontiera, M. G. Blaber, G. C. Schatz, and R. P. Van Duyne, "High-performance SERS substrates: Advances and challenges," *MRS Bull.*, vol. 38, no. 8, pp. 615–624, 2013, doi: 10.1557/mrs.2013.161.

ZHIBIN CHEN was born in Hunan, China, in June 1965. He received the Ph.D. degree in science from the Beijing University of Technology in 2005.

He is mainly engaged in electrical information detection and encryption transmission research.

MENGZE QIN was born Hebei, China, in November 1990. He received the B.Sc. degree from Hebei University in 2014 and the master's degree in engineering from Ordnance Engineering College in 2016.

He is currently studying with Army Engineering University at Shijiazhuang Campus and is mainly engaged in surface enhanced Raman scattering (SERS) applications research with attention to SERS's applications in explosives detection.

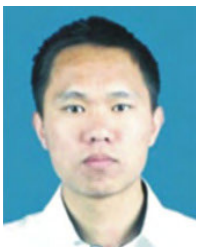

CHENG XIAO was born in Jiangsu, China, in 1989. He received the bachelor's degree in engineering from Nanjing University in 2008 and the Ph.D. degree in engineering from Army Engineering University in 2018.

He is currently studying with Army Engineering University and is mainly engaged in surface enhanced Raman scattering (SERS) applications research with attention to SERS's applications in explosives detection.